

Magnetic polaron conductivity in FeCr_2S_4 with the colossal magnetoresistance effect

Zhaorong Yang,* Shun Tan, Zhiwen Chen, and Yuheng Zhang

Structure Research Laboratory, University of Science and Technology of China, Academia Sinica,
Hefei, Anhui 230026, People's Republic of China

(Received 21 December 1999; revised manuscript received 14 June 2000)

The magnetic and electrical transport properties of the colossal magnetoresistance material FeCr_2S_4 are studied. Low-temperature thermoelectric power and resistivity measurements indicate that magnetic polarons dominate the conduction behavior at temperatures above T_c^{onset} . The temperature dependence of the susceptibility χ , measured from 4.2 to 400 K, suggests that FeCr_2S_4 is ferrimagnetic. Then the micromagnetism of FeCr_2S_4 is further investigated by electron-spin-resonance measurements from 100 to 290 K, which reveal that the paramagnetic-ferrimagnetic transition is incomplete and that a paramagnetic phase coexists with a ferrimagnetic phase in a certain temperature range below T_c^{onset} . Accompanying the paramagnetic-ferrimagnetic phase transition, magnetic polarons may delocalize gradually into the naked carriers. The resistivity in the presented temperature range can be described in terms of the two-fluid model concerning the coexistence of magnetic polarons and naked carriers.

Hole-doped manganite perovskites have become the focus of scientific and technological interest in the past several years, because they exhibit colossal magnetoresistance (CMR) effects.¹⁻³ A number of studies on these materials revealed that the spin, the charge, and the lattice in this system are strongly correlated. Within the framework of double-exchange (DE) and Jahn-Teller (JT) polarons, the CMR effect in this system can be explained qualitatively.⁴⁻⁸

Up to now two other CMR materials have been discovered— FeCr_2S_4 , with a spinel structure, and $\text{Tl}_2\text{Mn}_2\text{O}_7$, with a pyrochlore structure.^{9,10} Because the magnetotransport behaviors of FeCr_2S_4 and manganite perovskites are quite similar, one might expect to apply the DE theory and JT polaron mechanism to explain the CMR effects in FeCr_2S_4 . However, FeCr_2S_4 differs both structurally and electronically from the manganite perovskites.¹¹ In FeCr_2S_4 , there is neither heterovalence nor a JT polaron. Moreover, there is no appreciable structural discontinuity around the Curie temperature T_c . These facts strongly imply that FeCr_2S_4 belongs to a class of CMR system with a different underlying magnetoresistance mechanism.

FeCr_2S_4 was widely studied in the 1970s,¹²⁻¹⁶ but its CMR effects did not receive as much attention then.¹⁷ In this work, we perform resistivity, thermoelectric power, magnetization, and electron-spin-resonance measurements to study systematically the magnetic transport and CMR mechanism in this material. Our results suggest a magnetic polaron model for high-temperature conduction behavior. In a certain temperature range below T_c^{onset} , magnetic polarons coexist with naked carriers. Thus the resistivity can be reasonably explained within the framework of a two-fluid model.

The polycrystalline FeCr_2S_4 samples were prepared by standard solid-state synthesis method.⁹ The power x-ray-diffraction pattern showed that all observed peaks could be indexed with a cubic cell with $a = 0.99941(7)\text{nm}$, and a space group $Fd\bar{3}m$.¹⁸

The magnetization (M) measurements in the temperature range from 4.2 to 400 K were performed using a superconducting quantum interference device magnetometer in a

field-cooling (FC) and zero-field-cooling (ZFC) sequence under an applied field of 0.01 T, which is shown in Fig. 1(a). As seen from the $M-T$ curve, M increases with decreasing temperature, and then increases abruptly near T_c^{onset} (173 K) due to the paramagnetic-ferromagnetic (PM-FM) transition. The Curie temperature T_c (168 K) is defined as the temperature corresponding to maximum of $|dM/dT|$. In manganite perovskites, the decrease of magnetization with decreasing temperature may be indicative of the presence of magnetic order frustration or a transition into a spin-glass phase.^{19,20}

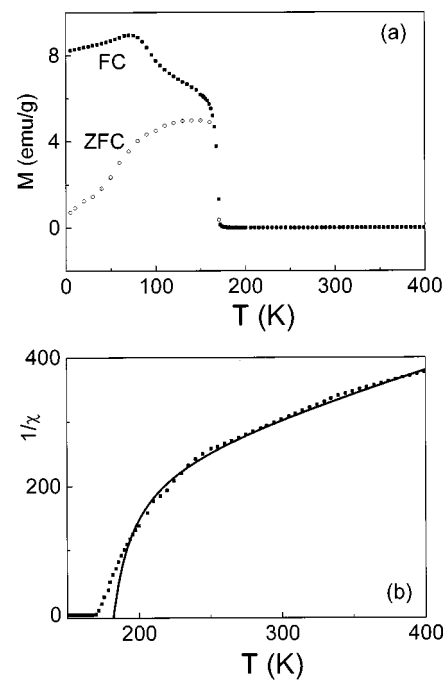


FIG. 1. (a). Temperature dependence of the magnetization ($M \sim T$) in FC and ZFC sequences respectively. (b) Temperature dependence of the paramagnetic susceptibility χ as a plot of $1/\chi$ vs temperature. The solid line is a fit to Eq. (1), with parameters given in the text.

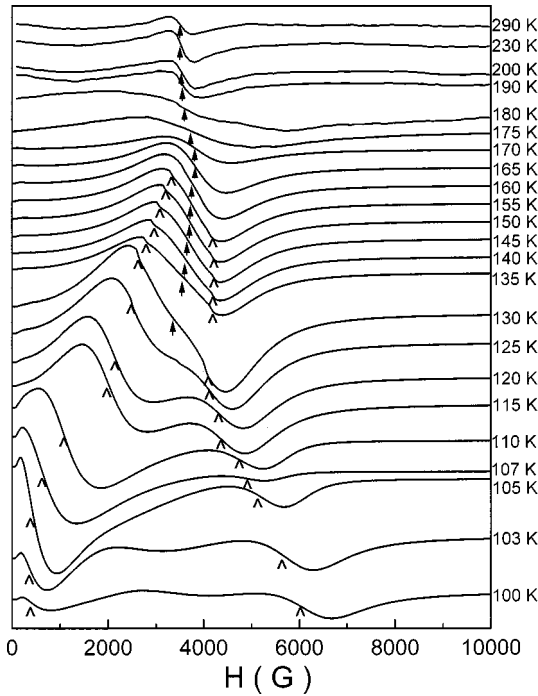


FIG. 2. ESR spectrum at different temperatures between 100 and 290 K. \uparrow marks the PM peak, and \wedge marks the FMR peak.

On the other hand, in a ferrimagnet, the above phenomena can also be attributed to spin-reorientation transitions.²¹ Then, in order to clarify the magnetism in FeCr_2S_4 , it is necessary to investigate the paramagnetic susceptibility. The temperature dependence of the paramagnetic susceptibility χ is shown in Fig. 1(b) as a plot of $1/\chi$ versus temperature, which is similar to the results reported by Srinivasan and Seehra.²¹ According to the physics of ferrimagnetism, as Srinivasan and Seehra pointed out, the temperature dependence of the paramagnetic susceptibility χ can be described by Eq. (1) (Refs. 21 and 22):

$$\frac{1}{\chi} = \frac{T}{C} + \frac{1}{\chi_0} - \frac{\sigma}{T - \theta} \quad (1)$$

Here χ_0 , C , σ , and θ are fitting parameters. The fit results of χ are shown as the solid line in Fig. 1(b), with $\theta = 167 (\pm 3)$, $\sigma = 3818 (\pm 50)$, $1/\chi_0 = 130 (\pm 2)$, and $C = 1.50 (\pm 0.02)$. Clearly, the experimental result fits Eq. (1) well except near T_c , indicating that the sample is a ferrimagnet. As is known, at temperatures near and above T_c , there is strong short-range magnetic correlation in system; thus the system is not in an ideal PM state, and the fit of Eq. (1) is not good near T_c . According to Néel's two-sublattice model,²² both the Fe sublattice and Cr sublattice are ferromagnetic, while the magnetic moment of the Fe sublattice is antiparallel to that of the Cr sublattice due to the magnetic coupling between these two sublattices.

Here we further investigate the micromagnetism of FeCr_2S_4 by the electron-spin-resonance (ESR) measurements. The ESR spectra of the powder sample were recorded from 100 to 290 K in a Bruker ER200D spectrometer at 9.4 GHz, as shown in Fig. 2. At temperatures above T_c^{onset} (173 K), only one ESR signal is observed, with g factor near 2, which is marked by the dark arrow. The signal can be

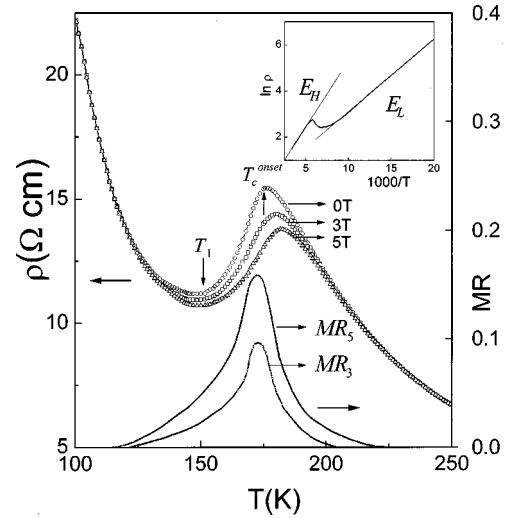


FIG. 3. Resistivity ρ and magnetoresistance $\text{MR}_H = [\rho(0) - \rho(H)]/\rho(0)$, vs temperature for FeCr_2S_4 . The inset shows the curve of $\ln \rho$ vs $1000/T$.

thought to originate from Fe and/or Cr ions. Below T_c^{onset} , as seen from Fig. 2, a ESR signal with a g factor near 2 still exists in the temperature range from T_c^{onset} to 155 K, which indicates that the PM-ferrimagnetic transition is incomplete, and that the PM phase may coexist with the ferrimagnetic phase. Clearly, the ESR spectrum splits, as shown in Fig. 2, and the splitting peaks (higher- and lower-field splitting peaks, marked by “ \wedge ”) are separated from the PM signals. The original PM peak is broadened gradually as the temperature is lowered, and eventually vanishes at about 125 K. The splitting peaks shift toward lower and higher fields with decreasing temperature, respectively. In a single-crystal sample, the shape of the sample and the direction of the magnetic field may determine whether the shift is positive or negative.²³ However, in our case, these effects of the powder sample have been averaged.²¹ Thus the two splitting peaks reflect the antiparallel magnetic moment between the Fe and Cr sublattices. Because the moment of the Cr sublattice is larger than that of the Fe sublattice, the moment of the Cr sublattice is likely to be parallel to the applied field. Hence the internal field of the Cr sublattice may cause its ferromagnetic resonance (FMR) line shift to lower fields, which forms the left branch peaks. So does the Fe sublattice, though it is antiparallel and forms right branch peaks.

The resistivity measurements were performed using a standard four-probe method in the temperature range from

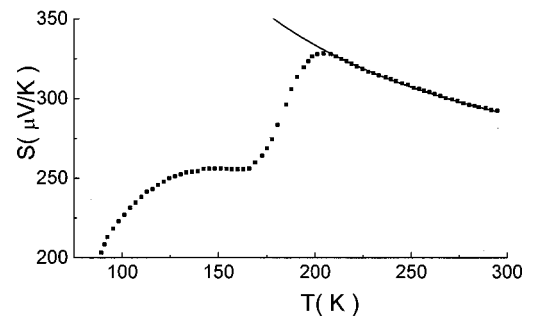


FIG. 4. Thermoelectric power (S) vs temperature for FeCr_2S_4 . The dark real line in (b) is fitted by $S = (k_B/e)(a + E_S/k_B T)$.

4.2 to 300 K under three different applied fields (0, 3, and 5 T). The resistivity ρ , and magnetoresistance $MR_H = [\rho(0) - \rho(H)]/\rho(0)$, as a function of temperature are shown in Fig. 3. Both ρ and MR_H display a peak near T_c^{onset} . The maximum of MR_5 is 16%. The temperature corresponding to the minimum resistivity in the $\rho \sim T$ curve below T_c is defined as T_1 (=153 K). It is interesting that T_1 is just the temperature corresponding to ESR spectra splitting. As seen from the inset of Fig. 3, the curve of $\ln \rho$ versus $1000/T$ is linear at both $T > T_c^{\text{onset}}$ and $T < T_1$, indicating a semiconductorlike behavior in two regions. The fits by $\rho = \rho_0 \exp(E/k_B T)$ give the activation energies $E_L = 26$ meV for $T < T_1$, and $E_H = 47$ meV for $T > T_c^{\text{onset}}$, respectively. This implies that the conduction mechanisms are different for the two temperature regions.

$E_H > E_L$ indicates clearly that E_H , the activated energy at temperatures above T_c^{onset} , does not arise from a simple thermally activated effect. In order to understand the discrepancy between E_L and E_H , we performed a thermoelectric power (S) measurement, which is shown in Fig. 4. Fitting the experimental data by $S = (k_B/e)(a + E_S/k_B T)$,²⁴ we obtain 23 meV for E_S , which is approximately equal to 26 meV for E_L , and much lower than 47 meV for E_H . In manganite perovskites, the discrepancy between E_S and E_H can be attributed to the presence of lattice or magnetic polarons. However, in our case, as there is neither a structure transition around T_c nor a JT effect, the polarons mainly exist in the form of magnetic polarons.²⁵

It can be seen in Fig. 2 that the sample is in a typical PM state at temperatures above T_c^{onset} , which is favorable for the existence of magnetic polarons. As we know, a magnetic polaron is a carrier coupled by short-range magnetic correlation within a magnetic cluster at temperatures above T_c^{onset} . Accordingly, the effective mass of a magnetic polaron increases greatly with respect to that of a naked carrier; therefore, a magnetic polaron has a lower mobility and a higher activated energy.^{26–28}

Note that the paramagnetic-ferrimagnetic transition takes place at T_c^{onset} . Magnetic polarons will be delocalized from the self-trapped state and turn into naked carriers completely in an ideal ferrimagnetic order.^{26,27} As a consequence, the

resistivity decreases drastically at this point, and the system should change completely to one of thermal activation transport of naked carriers. However, the resistivity decreases gradually with temperature from T_c^{onset} to T_1 , and MR also extends to a broader temperature range below T_c^{onset} (as seen from Fig. 3). This indicates that magnetic polarons may still exist in this temperature range. It is noted in Fig. 2 that ESR signals with g factor near 2 also exist in the temperature range from T_1 to T_c^{onset} . This indicates that a PM state still exists at this temperature range, which provides a survival environment for the magnetic polaron. Magnetic polarons will be delocalized gradually as the PM phase weakens. They then vanish completely at T_1 , denoting that magnetic order destroys the environment for magnetic polarons. Thus the resistivity in the temperature range could be attributed to two factors: the thermal activation effect and the transport of magnetic polarons. Thus the resistivity in the presented temperature range can be described in terms of a two-fluid model concerning the coexistence of magnetic polarons and naked carriers. An external magnetic field will increase the ferrimagnetic order, and inhibit the formation of magnetic polarons, thus MR extends to a broader temperature range below T_c^{onset} .

In conclusion, the magnetic and transport properties of FeCr_2S_4 are studied in detail. The experimental results for thermoelectric power measurement suggest a magnetic polaron conduction at temperatures above T_c^{onset} . The temperature dependence of the ESR signal indicates that a PM phase coexists with a ferrimagnetic phase in a certain temperature range just below T_c^{onset} , and suggests that magnetic polarons may coexist with delocalized carriers in that temperature range. Accordingly, the resistivity in the presented temperature range can be described in terms of a two-fluid model concerning the coexistence of magnetic polarons and naked carriers.

We thank Associate Professor Yunhua Xu for the ESR measurements. This work was supported by the National Natural Science Foundation of China and the Foundation of Academia Sinica, People's Republic of China, as well as the Research Fund for the Doctoral Program of Higher Education.

*Corresponding author. Email address: yzr@mail.usc.edu.cn

¹K. Chahara, T. Ohno, M. Kassai, and Y. Kozono, *Appl. Phys. Lett.* **63**, 1990 (1993).

²R. Von Helmolt, J. Wecker, B. Holzapfel, L. Schultz, and K. Samwer, *Phys. Rev. Lett.* **71**, 2331 (1993).

³S. Jin, T. H. Tiefel, M. McCormack, R. A. Fastnacht, R. Ramesh, and J. H. Chen, *Science* **264**, 413 (1994).

⁴C. Zener, *Phys. Rev.* **82**, 403 (1951).

⁵P. G. de Gennes, *Phys. Rev.* **118**, 141 (1960).

⁶A. Asamitsu, Y. Moritomo, Y. Tomioka, T. Arima, and Y. Tokura, *Nature (London)* **373**, 407 (1995).

⁷A. J. Millis, P. M. Littlewood, and B. I. Shraiman, *Phys. Rev. Lett.* **74**, 5144 (1995).

⁸M. R. Ibarra, P. A. Algarabel, C. Marquina, J. Blasco, and J. Garcia, *Phys. Rev. Lett.* **75**, 3541 (1995).

⁹A. P. Ramirez, R. J. Cava, and J. Krajewski, *Nature (London)* **386**, 156 (1997).

¹⁰M. A. Subramanian, B. H. Toby, A. P. Ramirez, W. J. Marshall, A. W. Sleight, and G. H. Kwei, *Science* **273**, 81 (1996).

¹¹Z. W. Chen, S. Tan, Z. R. Yang, and Y. H. Zhang, *Phys. Rev. B* **59**, 11 172 (1999).

¹²G. Haacke and L. C. Beegle, *J. Appl. Phys.* **39**, 656 (1968).

¹³P. Gibart, J. L. Dormann, and Y. Pellerin, *Phys. Status Solidi* **36**, 187 (1969).

¹⁴P. Gibart, M. Robbins, and V. G. Lambrecht, *J. Phys. Chem. Solids* **34**, 1363 (1973).

¹⁵T. Watanabe and I. Nakada, *Jpn. J. Appl. Phys.* **17**, 1745 (1978).

¹⁶J. B. Goodenough, *J. Phys. Chem. Solids* **30**, 261 (1969).

¹⁷L. Goldstein and P. R. Gibart, in *Magnetism and Magnetic Materials*, edited by D. C. Graham and J. J. Rhyne, AIP Conf. Proc. No. 5 (AIP, New York, 1971), p. 883

¹⁸L. Shi, Q. Z. Dong, Z. R. Yang, Z. W. Chen, and Y. H. Zhang, *Chin. Phys. Lett.* **16**, 532 (1999).

¹⁹K. Binder and A. P. Young, *Rev. Mod. Phys.* **58**, 801 (1986).

- ²⁰X. X. Zhang, R. H. Yu, J. Tejada, G. F. Sun, Y. Xin, and K. W. Wong, *Appl. Phys. Lett.* **68**, 22 (1996).
- ²¹G. Srinivasan and Mohindar S. Seehra, *Phys. Rev. B* **28**, 1 (1983).
- ²²L. Néel, *Ann. Phys. (Paris)* **3**, 137 (1952).
- ²³D. L. Huber and M. S. Seehra, *Phys. Status Solidi B* **74**, 145 (1976).
- ²⁴M. F. Hundley and J. J. Neumeier, *Phys. Rev. B* **55**, 11 511 (1997).
- ²⁵A. P. Ramirez, *J. Phys.: Condens. Matter* **9**, 8171 (1997).
- ²⁶Mark Rubinstein, D. J. Gillespie, John E. Snyder, and Terry M. Tritt, *Phys. Rev. B* **56**, 5412 (1997).
- ²⁷R. M. Kusters, J. Singleton, D. A. Keen, R. McGreevy, and W. Hayes, *Physica B* **155**, 362 (1989).
- ²⁸Y. Shapira, S. Foner, N. F. Oliveira, and T. B. Reed, *Phys. Rev. B* **10**, 4765 (1974).